Synthesis of Network Polymers Composed of Well-Defined Silyl Ether Macrocycles

Chihiro Nakai,‡[a] Sota Amano,‡[a] Koh Sugamata,[b,c] Naoki Watanabe,[d] Hiroaki Imoto,[a] Kensuke Naka,[a] Takahiro Iwamoto.*[a]

Faculty of Molecular Chemistry and Engineering, Kyoto Institute of Technology, Goshokaido-cho, Matsugasaki, Sakyo-ku, Kyoto 606-8585, Japan

Department of Chemistry, Institute of Pure and Applied Sciences, University of Tsukuba, 1-1-1 Tennoudai, Tsukuba, Ibaraki 305-8571, Japan

Tsukuba Research Center for Energy Materials Sciences (TREMS), University of Tsukuba, 1-1-1 Tennoudai, Tsukuba, Ibaraki 305-8571, Japan

JNC Petrochemical Corporation, 5-1, Goikaigan, Ichihara, Chiba 290-8551, Japan

E-mail: tiwamoto@kit.ac.jp

Contents

1. General Considerations
2. Synthetic Experimental
3. Film fabrication
4. Single Crystal X-ray Analyses
5. References
6. NMR Spectra

1. General Considerations

^{1}H (400 MHz), ^{13}C (100 MHz), and ^{29}Si (80 MHz) nuclear magnetic resonance (NMR) spectra were obtained using a Bruker AVANCE III 400 NMR spectrometer (Bruker Biospin GmbH, Rheinstetten, Germany) in $CDCl_3$ using residual $CHCl_3$ as an internal standard. The ^{13}C chemical shifts are referenced to signals of $CDCl_3$ (δ 77.16). High-resolution mass (HRMS) spectra were obtained with a Bruker timsTOF APCI-QTOF atmospheric pressure chemical ionization (APCI). Fourier transform infrared (FT-IR) spectra were obtained on a JASCO FT/IR-4600 (JASCO, YoungTokyo, Japan) spectrometer using attenuated total reflection method and KBr plates method. Thermogravimetric analysis (TGA) and differential scanning calorimetry (DSC) measurements were performed by Shimadzu DTG-60 and DSC-60 Plus (Shimadzu), respectively, under N_2 atmosphere. Scanning electron microscopy (SEM) images were obtained using a VE-8800 microscope (KEYENCE, Osaka, Japan). Elastic modulus measurements of the cast films were performed using a Shimadzu DUH-211 instrument. Static water contact angles for the cast films were measured with DMs-301/401 (Kyowa Interface Science, Saitama, Japan) at 25 °C by using water (1.0 μL) as a probe fluid. Each contact angle is reported as the average value of four independent measurements. UV-vis absorption spectra were recorded on a JASCO spectrophotometer V-670 KNN (JASCO, Tokyo, Japan).

2. Synthetic Experimental

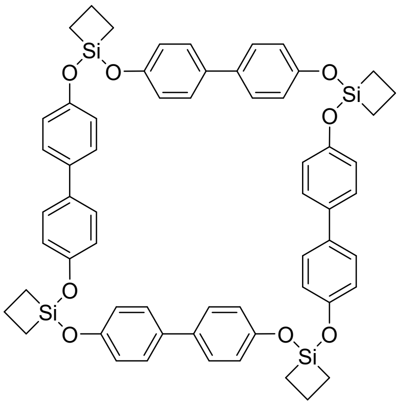

Synthesis of macrocycle 2

To a solution of 4,4'-dihydroxybiphenyl (47.6 mg, 0.256 mmol) and imidazole (34.6 mg, 0.508 mmol) in THF (1.0 mL) was added 1,1-dichlorosilacyclobutane (30 μL, 0.256 mmol). After the mixture was stirred at room temperature for 30 mins, the resulting suspension was filtered, and the solid was washed with THF. The solvent was removed under reduced pressure to afford the crude product. The crude product was dissolved in CH_2Cl_2, then precipitated by CH_3CN, followed by filtration to afford the title product (58.8 mg, 0.058 mmol) in 90% yield.

^{1}H NMR ($CDCl_3$) δ 7.43 (d, J = 8.5 Hz, 16H), 7.02 (d, J = 8.6 Hz, 16H), 1.88–1.77 (m, 8H), 1.77–1.68 (m, 16H); ^{13}C NMR ($CDCl_3$) δ 152.6, 135.0, 128.0, 119.9, 21.7, 11.7; ^{29}Si NMR (DEPTSi, 79MHz, $CDCl_3$) δ −20.9; HRMS (APCI): *m/z* $[M]^+$ calcd for $C_{60}H_{56}O_8Si_4$ 1016.3047, found 1016.3029; IR (ATR): v = 3033, 2978, 2933, 1601, 1491, 1399, 1387, 1225, 1165, 1121, 1027, 927, 850, 824, 777, 715, 643, 626, 617, 553, 522 cm^{-1}. mp: 155–178 °C.

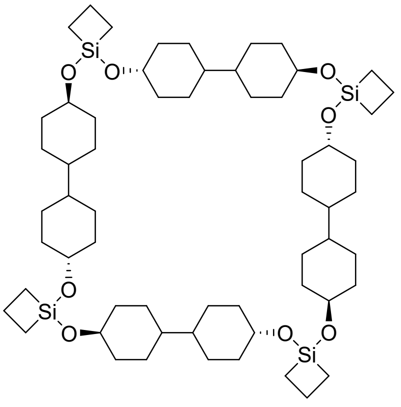

Synthesis of macrocycle 4

To a solution of 4,4'-bicyclohexanediol (52.6 mg, 0.265 mmol) and imidazole (34.7 mg, 0.510 mmol) in THF (1.0 mL) was added 1,1-dichlorosilacyclobutane (30 μL, 0.256 mmol). After the mixture was stirred at 0 °C for 10 mins and then at room temperature for 30 mins, the resulting suspension was filtered, and the solid was washed with THF. The solvent was removed under reduced pressure to afford the almost pure title product (69.8 mg, 0.065 mmol) in 99% yield.

^{1}H NMR ($CDCl_3$) δ 3.76 (m, 8H), 2.01–1.92 (m, 16H), 1.80–1.61 (m, 24 H), 1.46–1.27 (m, 32H), 1.10–0.92 (m, 24H); ^{13}C NMR ($CDCl_3$) δ 72.3, 41.8, 36.1, 28.6, 21.8, 12.0; ^{29}Si NMR (DEPTSi, 79MHz, $CDCl_3$) δ −21.1; Although HRMS measurements could not be obtained due to difficulties in ionization, the NMR spectra of the crystals used for the single-crystal X-ray diffraction analysis were identical to those described above, confirming that the structure is correctly assigned; IR (ATR): v = 2925, 2854, 1449, 1379, 1122, 1059, 985, 956, 895, 845, 813, 791, 703, 622, 528 cm^{-1}.

Polymerization of macrocycle 2 via ring opening reaction of silacyclobutane

Differential scanning calorimetry (DSC) measurements were conducted under a nitrogen atmosphere. Macrocycle **2** (3.6 mg) were loaded into aluminum pans and heated from 30 to 350 °C at a heating rate of 10 °C min^{-1}, followed by an isothermal hold at 350 °C for 2 h (**Figure 2a**). Prior to the measurements, the samples were dried under vacuum. Since no phase transition was observed in the second scan, the reaction is considered to have completed during the first heating scan (**Figure S3**).

The peak of the reference compound **5** at approximately 1121 cm^{-1} in the FT-IR spectrum remained essentially unchanged. This confirms that the disappearance of the 1127 cm^{-1} band originates from the reaction of the silacyclobutane units.

To verify that the ATR measurements were not limited to surface information, transmission FT-IR spectra were also recorded. These spectra exhibited comparable spectral changes, demonstrating that the silacyclobutane units located in the bulk interior likewise underwent smooth ring-opening reactions (Figure S2).

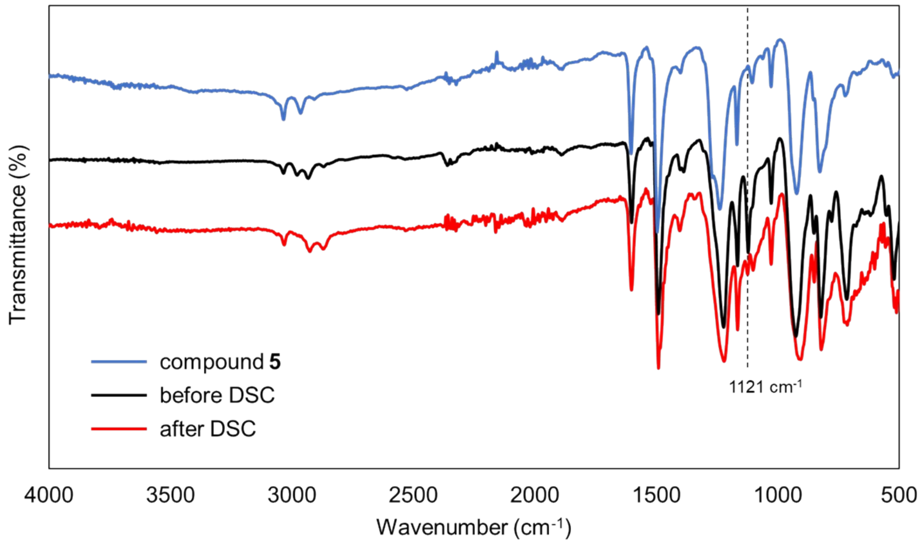

Figure S1. ATR FT-IR spectra of the samples after DSC measurements. (Full spectra of **Figure 2a**)

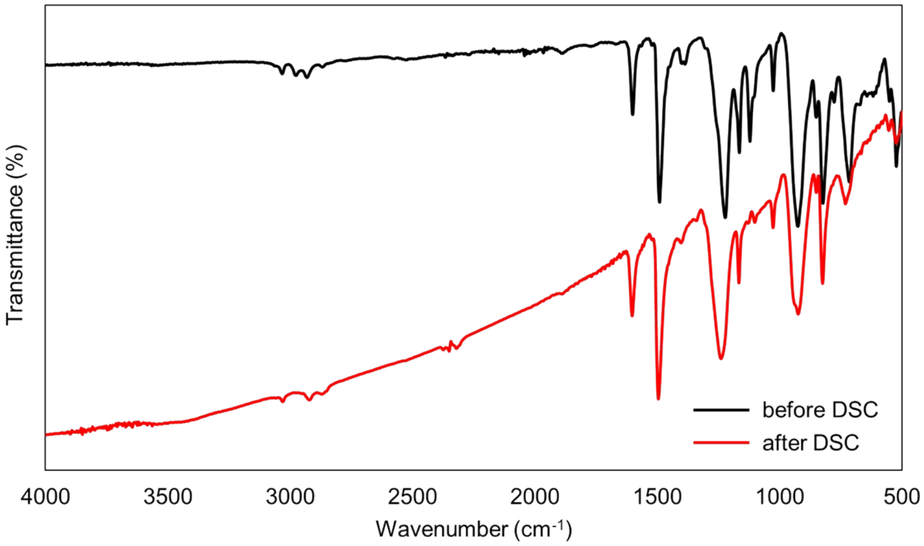

Figure S2. FT-IR spectra of the samples after DSC measurements measured by transmission mode using KBr plates.

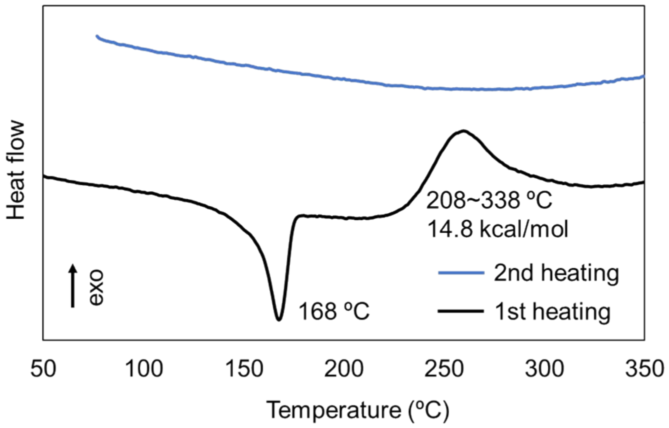

Figure S3. DSC analysis of the 1st (black) and 2nd (blue) heating scans.

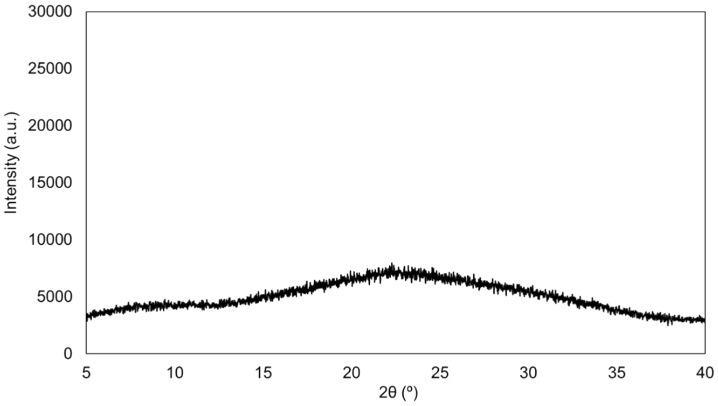

Figure S4. DSC measurements of the sample held at 160 °C for 3 h prior to thermal polymerization. During the isothermal holding, microparticles were generated and a new endothermic peak corresponding to their melting was observed. However, PXRD analysis of the DSC-treated sample showed no clear crystallinity.

Polymerization of macrocycle 4 via ring opening reaction of silacyclobutane

DSC measurements were conducted under a nitrogen atmosphere. Macrocycle **4** (1.5 mg) were loaded into aluminum pans and heated from 30 to 350 °C at a heating rate of 10 °C min^{-1}, followed by an isothermal hold at 350 °C for 2 h (**Figure 2b**). Prior to the measurements, the samples were dried under vacuum. Since no phase transition was observed in the second scan, the reaction is considered to have completed during the first heating scan (**Figure S7**). The transmission spectra were in good agreement with the ATR spectra, indicating smooth ring-opening reaction in the bulk interior. (**Figure S6**)

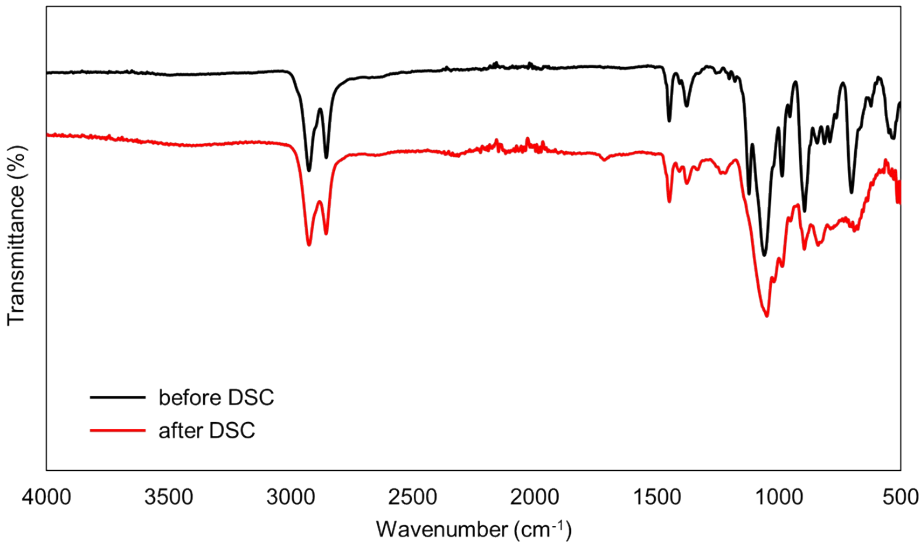

Figure S5. ATR FT-IR spectra of the samples after DSC measurements. (Full spectra of **Figure 2b**)

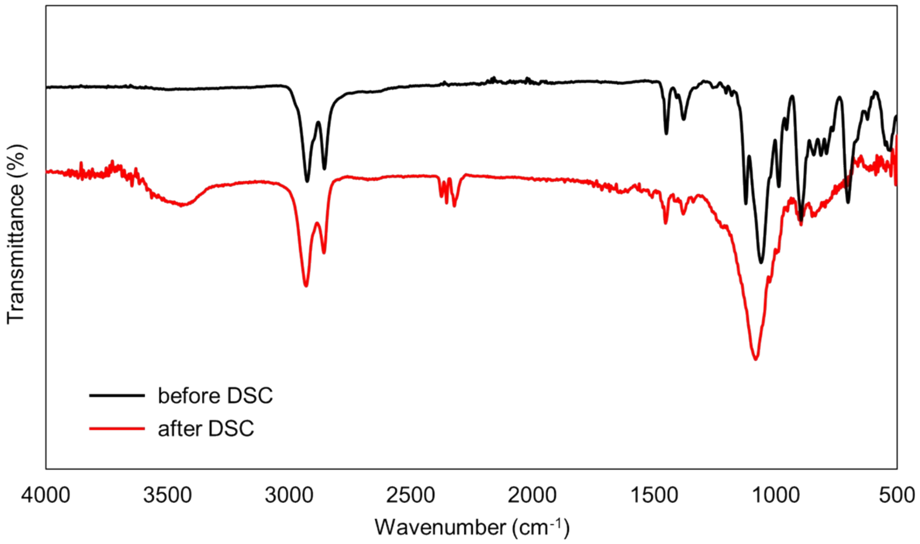

Figure S6. FT-IR spectra of the samples after DSC measurements measured by transmission mode using KBr plates.

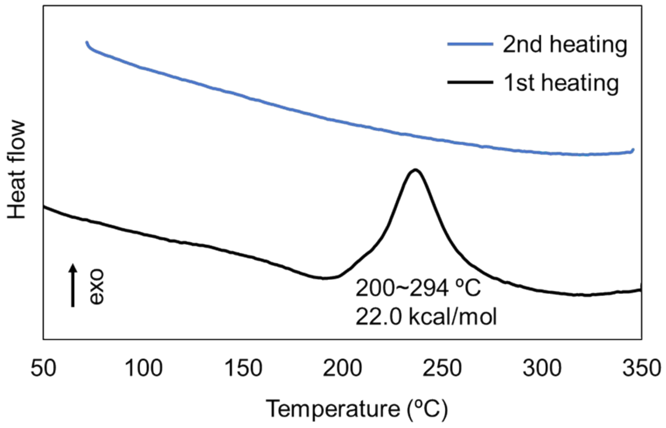

Figure S7. DSC analysis of the 1st (black) and 2nd (blue) heating scans.

Thermal stabilities of macrocycle 2 and 4

The sample masses were 3.1 mg and 4.0 mg, respectively. The measurements were carried out under a nitrogen atmosphere at a heating rate of 10 °C min^{-1}. TGA measurements of compounds **2** and **4** revealed no weight loss within the reaction temperature range.

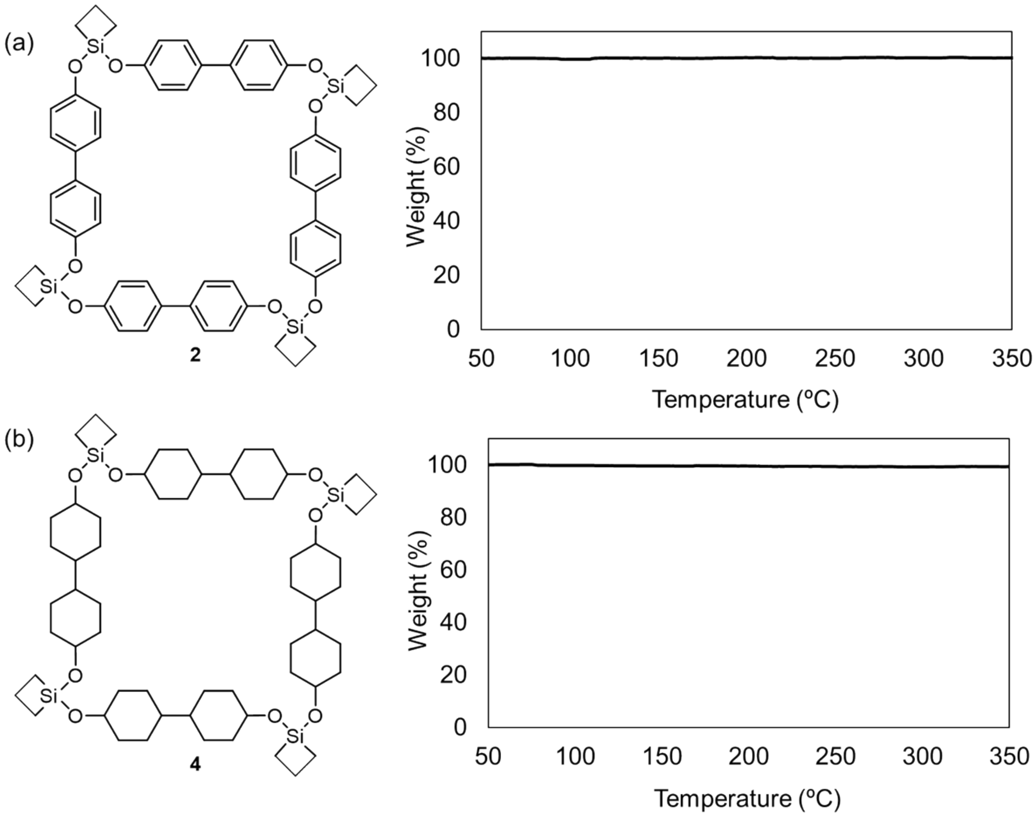

Figure S8. TGA curves of compounds **2** and **4**. No weight loss was observed within the reaction temperature range.

Thermal stabilities of macrocycle 5 and 6

The sample masses were 7.9 mg and 1.9 mg, respectively. The measurements were carried out under a nitrogen atmosphere at a heating rate of 10 °C min^{-1}. The data demonstrate that the macrocycle backbone persists without decomposition within the temperature window relevant to the silacyclobutane ring-opening process. The weight losses of macrocycle **5** and **6** at the temperatures at which the silacyclobutane ring-opening reaction is completed—338 °C for the biphenylene linker and 204 °C for the dicyclohexylene linker—were 4.2% and 4.1%, respectively.

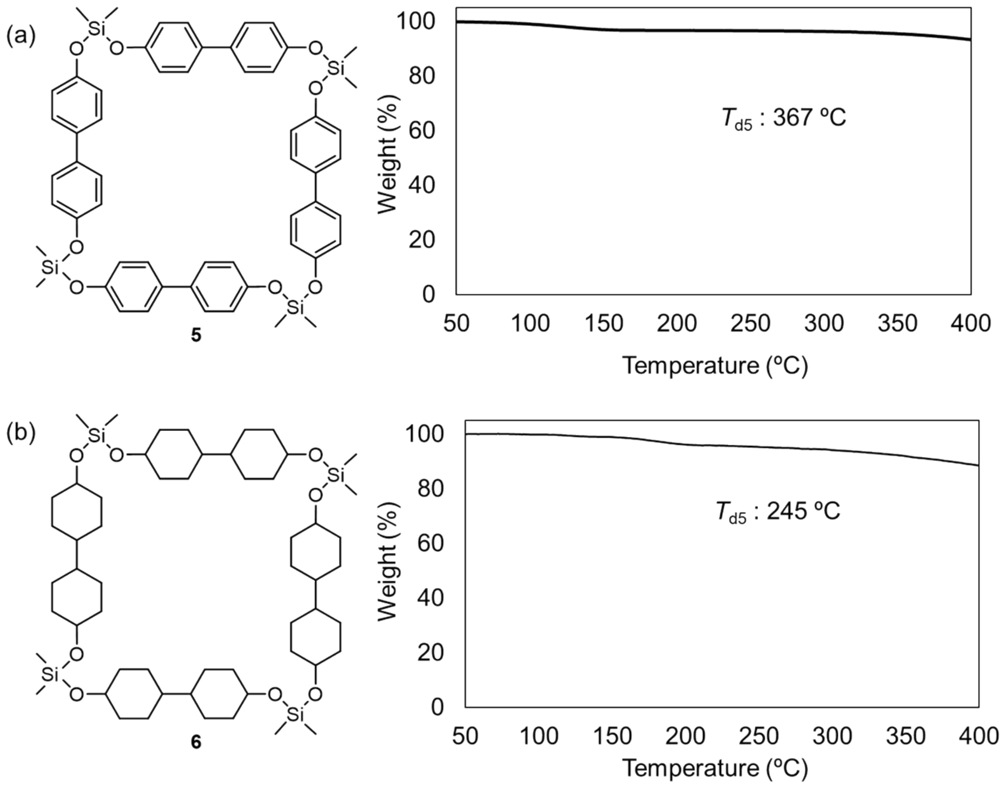

Figure S9. TGA curves of (a) macrocycle **5** and (b) macrocycle **6**. The 5% weight-loss temperatures (T_{d5}) were 367 °C and 245 °C, respectively.

3. Film fabrication

A Benzene solution (1.0 mL) of macorocyclic compound (1.0 mg) was cast onto a glass substrate, and kept for 24 h until the solvent was completely evaporated. The cased sample was heated at 255 °C for 1 h under argon atmosphere. In the film samples as well, FT-IR analysis confirmed the consumption of the silacyclobutane units, and PXRD showed no distinct diffraction peaks.

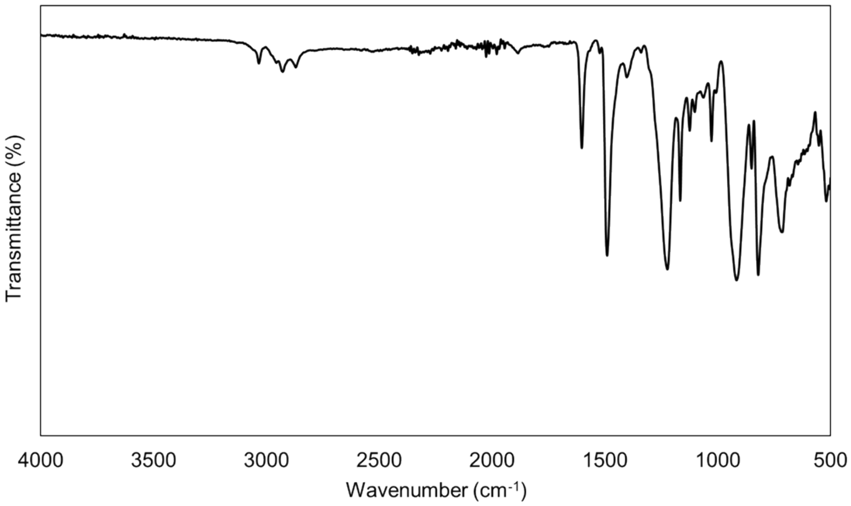

Figure S10. FT-IR spectra of film A.

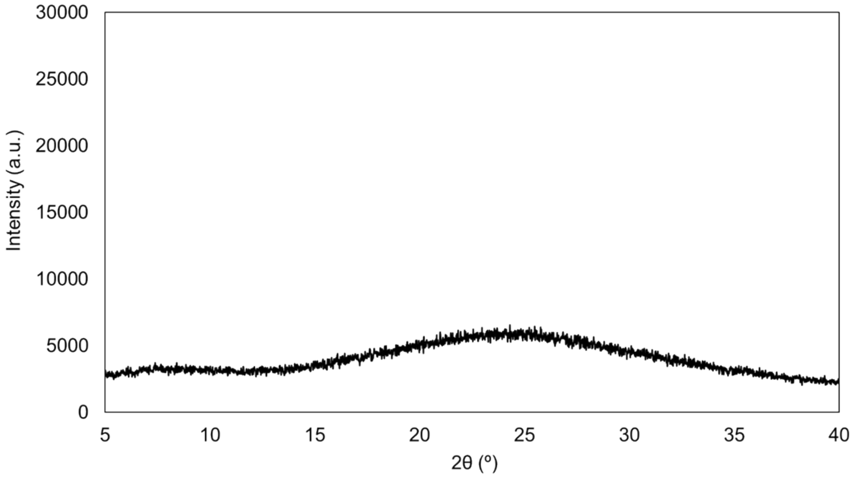

Figure S11. Powder X-ray diffraction pattern of film A.

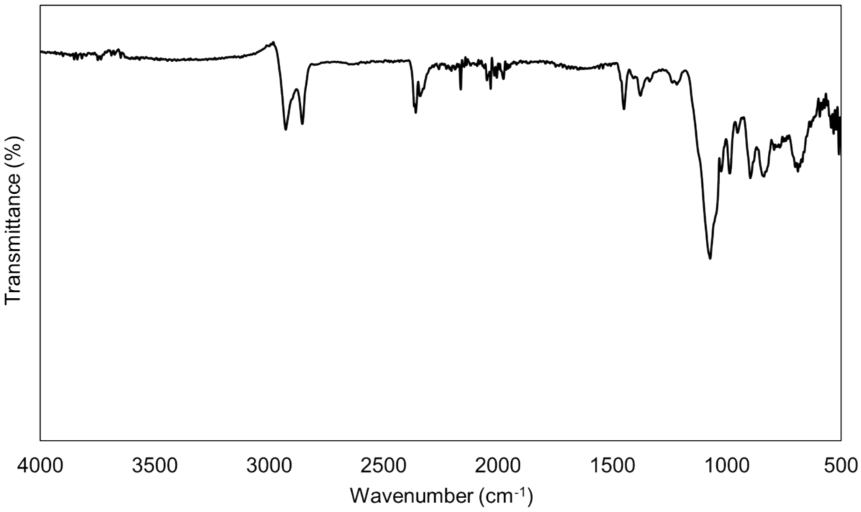

Figure S12. FT-IR spectra of film B.

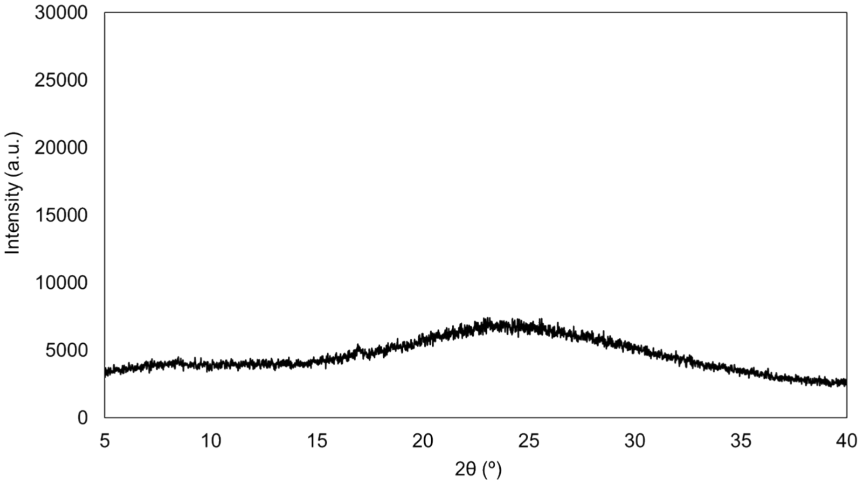

Figure S13. Powder X-ray diffraction pattern of film B.

Decomposition of film A

□□The degradation experiments were performed by immersing the film in a mixed solvent system consisting of an aqueous solution (1 mL) and ethanol (1 mL) for 24 h. Under acidic conditions, 1 N HCl (aq) was used as the aqueous component, whereas under neutral conditions, water was used. No noticeable decomposition was observed under neutral conditions. Even under acidic conditions, the film underwent only partial decomposition, with approximately 34% degradation after 24 h, leaving a substantial insoluble residue. The IR spectrum of the residual solid and the NMR spectrum of the decomposed fraction are presented to elucidate the decomposition behavior. The ^{1}H NMR spectrum of the decomposed fraction revealed characteristic signals of compound **1**.

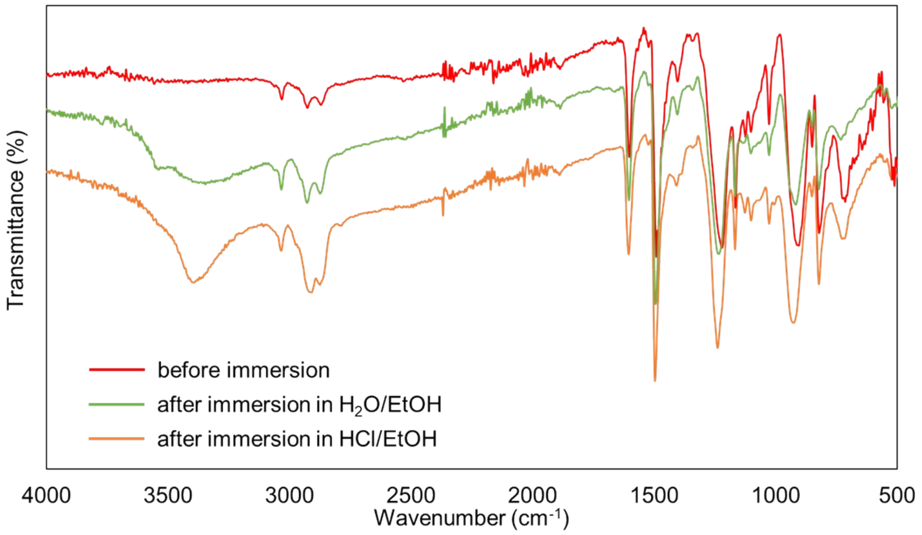

Figure S14. IR spectrum of the insoluble residue obtained after treatment of the film under acidic conditions (1 N HCl (aq)/ethanol, 24 h) or neutral conditions (H_2O/EtOH, 24 h).

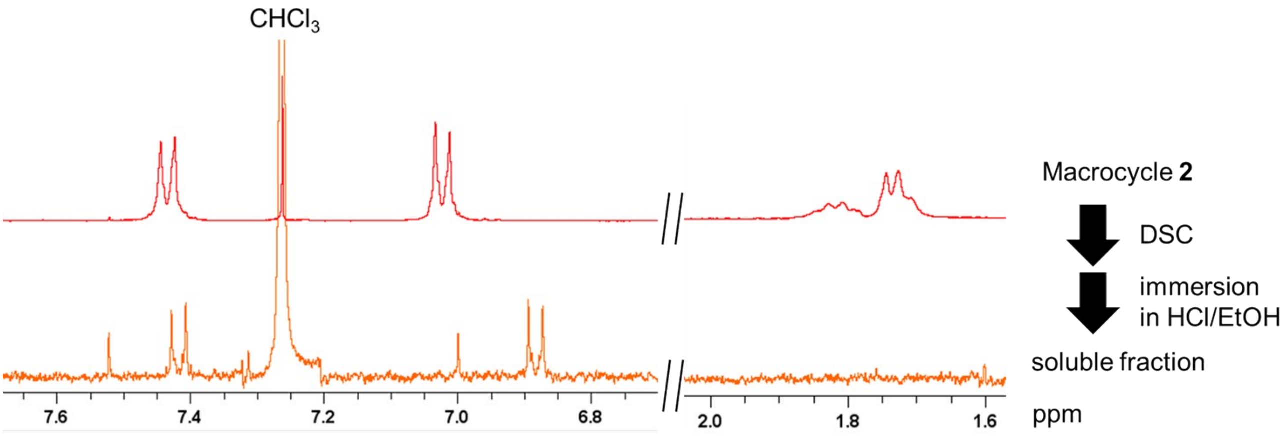

Figure S15. ^{1}H NMR spectrum of the soluble fraction obtained after acidic treatment of the film (1 N HCl (aq)/ethanol, 24 h).

Decomposition of film B

□□The same immersion test was conducted for film B. A 34% weight loss was observed in H_2O/EtOH after 24 h, while a significantly greater weight loss of 71% was observed in HCl (aq)/EtOH.

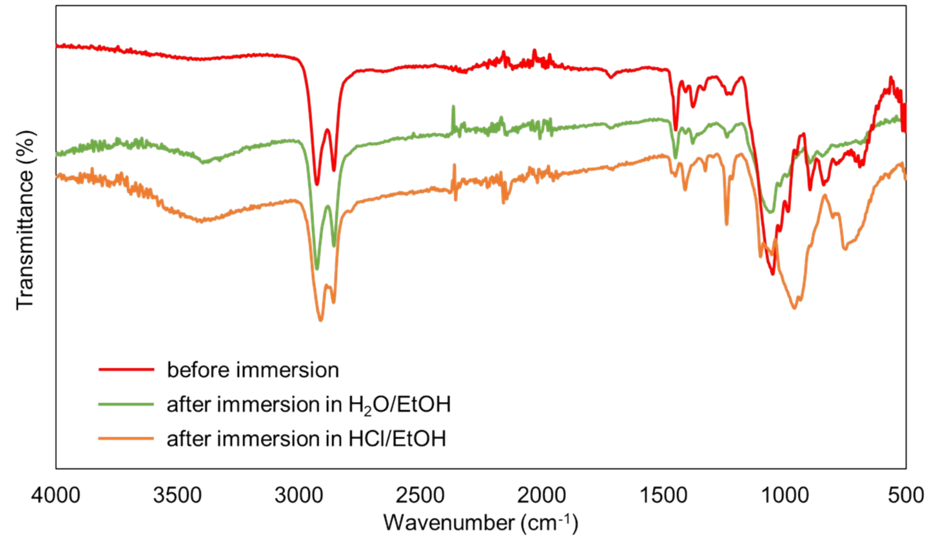

Figure S16. IR spectrum of the insoluble residue obtained after treatment of the film under acidic conditions (1 N HCl (aq)/ethanol, 24 h) or neutral conditions (H_2O/EtOH, 24 h).

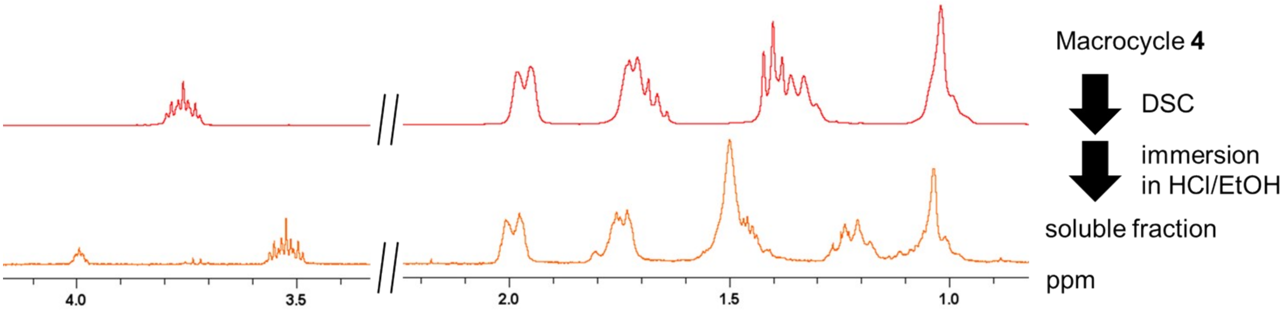

Figure S17. ^{1}H NMR spectrum of the soluble fraction obtained after acidic treatment of the film (1 N HCl (aq)/ethanol, 24 h).

Gas Sorption Measurements

Prior to the measurements, the film samples were dried at 60 °C for 1 h and then transferred to the sample cell for gas sorption analysis. Nitrogen adsorption isotherms were measured at 77 K to evaluate the adsorption behavior and possible surface area of the films. Carbon dioxide adsorption isotherms were measured at rt to examine the presence of microporosity.

In both N_2 (77 K) and CO_2 (room temperature) measurements, only very small gas uptake was observed within the accessible pressure range, indicating the absence of significant permanent porosity in the polymer films.

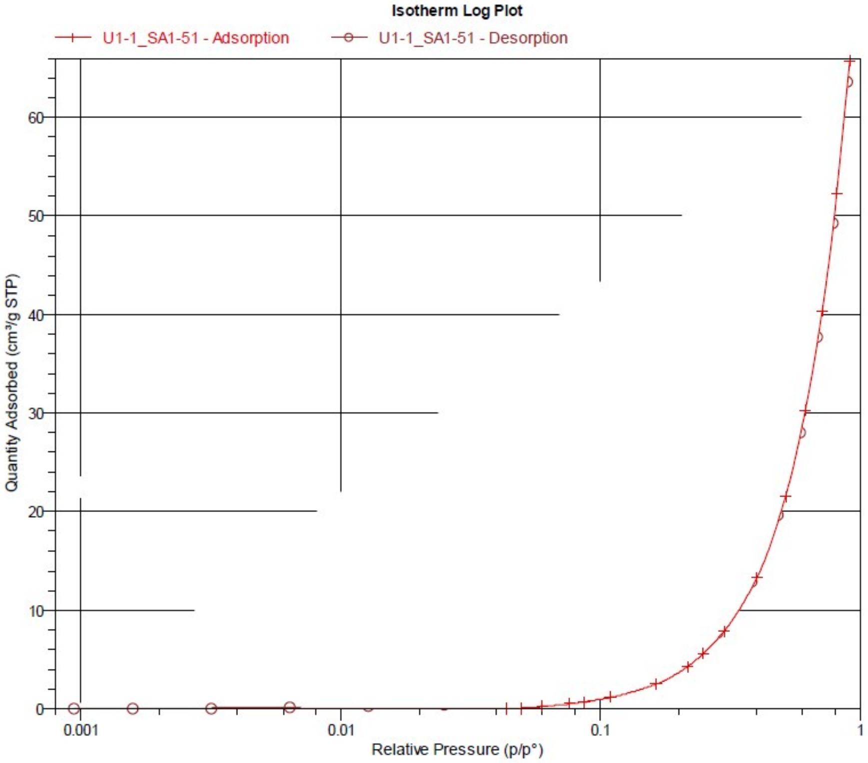

Figure S18. Nitrogen adsorption–desorption isotherms of the polymer films measured at 77 K after drying at 60 °C for 1 h. The films exhibit negligible N_2 uptake over the measured pressure range, indicating the absence of significant permanent porosity.

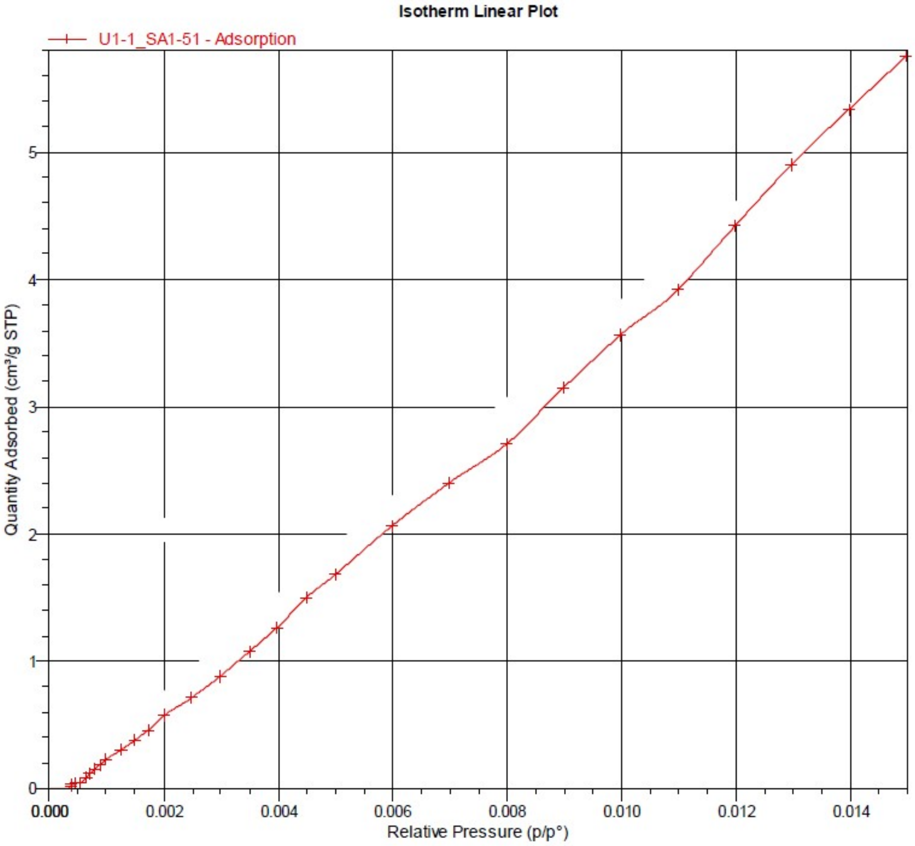

Figure S19. Carbon dioxide adsorption isotherms of the polymer films measured at room temperature (ca. 298 K) after drying at 60 °C for 1 h. Only minimal CO_2 uptake was observed, suggesting that the polymer network does not contain appreciable microporosity.

4. Single Crystal X-ray Analyses

Single-crystal X-ray diffraction data of **4** was collected on the BL02B1 beamline of SPring-8 (proposal numbers: 2025B1561, 2025B1719, 2025B1581, 2025A1949, 2025A1823, 2024A1857) on a PILATUS3 X CdTe 1M camera using synchrotron radiation (λ = 0.4132 Å). The structure was determined by intrinsic phasing (SHELXT 2018/2)[S1] and refined by full-matrix least-squares refinement (SHELXL-2018/3)[S2] using the yadokari[S3] software package. The disordered non-coordinated solvents were removed using the PLATON SQUEEZE program.[S4]

Selected distances are shown in Å. (c) Conformations of Ar–O–Si–O–Ar with their notations.

Single-crystal X-ray diffraction analysis was conducted in order to confirm the overall macrocyclic topology. Although the data clearly support the proposed connectivity and macrocyclic framework, the crystal quality was insufficient for accurate determination of bond parameters and full refinement. Accordingly, the crystallographic data were not deposited in the CCDC and are presented in the Supporting Information solely for qualitative discussion.

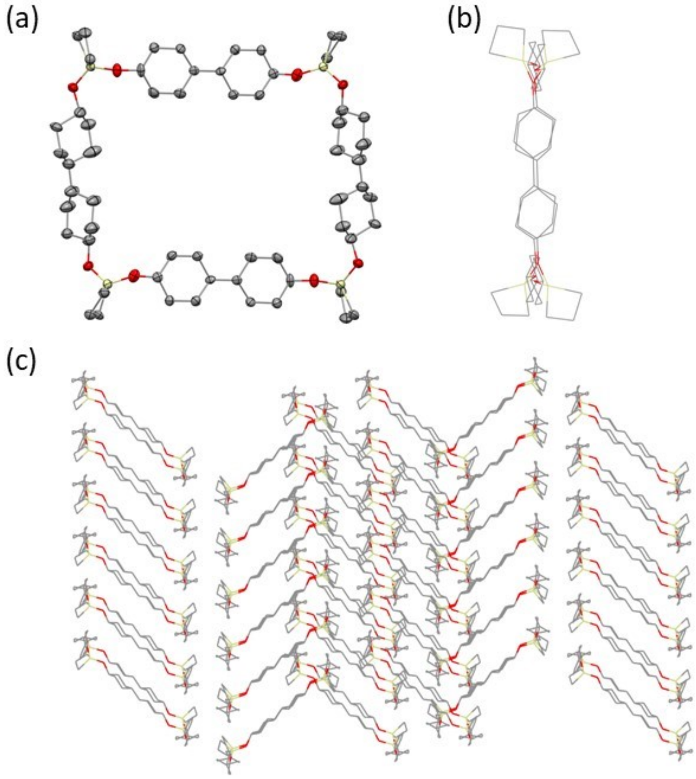

Figure S20. X-ray structures of macrocycle **4**. (a) Top view, (b) side view, and packing structures.

Table S1. X-ray Crystallographic Data for **4**.

	4
CCDC	Not deposited
formula	C60 H104 O8 Si4
fw	1065.79
crystal dimension (mm)	0.01 × 0.01 × 0.01
crystal system	monoclinic
space group	C 1 2/c 1
a, Å	56.165(9)
b, Å	5.7285(2)
c, Å	31.418(5)
α, deg	90
β, deg	140.12(3)
γ, deg	90
V, Å^3	6482(3)
Z	4
ρ_{calcd}, g cm^{-3}	1.092
F(000)	2336
index range	$-66 \leq h \leq 66$

	$-6 \le k \le 6$
	$-37 \le l \le 37$
no. reflections total	54376
no. parameters	426
$R1$ ($I > 2\sigma(I)$)[a]	0.1328
$wR2$ (all data)[b]	0.4358
GOF [c]	1.905
max diff peak / hole, e Å^{-3}	1.738/-0.670

[a] $R1 = \Sigma||F_o| - |F_c||/\Sigma|F_o|$. [b] $wR2 = [\Sigma\{w(F_o^2 - F_c^2)^2\}/\Sigma w(F_o^2)^2]^{1/2}$, $w = 1/[\sigma^2 F_o^2 + (aP)^2 + bP]$ (a and b are constants suggested by the refinement program; $P = [\max(F_o^2,0) + 2F_c^2]/3$). [c] $\mathrm{GOF} = [\Sigma w(F_o^2 - F_c^2)^2/(N_{\mathrm{obs}} - N_{\mathrm{params}})]^{1/2}$.

5. References

S1. Sheldrick, G. M. *Acta Crystallogr. Sect. A,* **2015**, *71*, 3-8.

S2. Sheldrick, G. M. *Acta Crystallogr. Sect. C,* **2015**, *71*, 3-8.

S3. Yadokari-XG, Software for Crystal Structure Analyses, K. Wakita (2001); Release of Software (Yadokari-XG 2009) for Crystal Structure Analyses, C. Kabuto, S. Akine, T. Nemoto, and E. Kwon, *J. Cryst. Soc. Jpn.,* **2009**, *51*, 218-224 (2009).

S4. Spek, A. L. *Acta Cryst. Sect. D,* **2009**, *65*, 145-155.

6. NMR Spectra

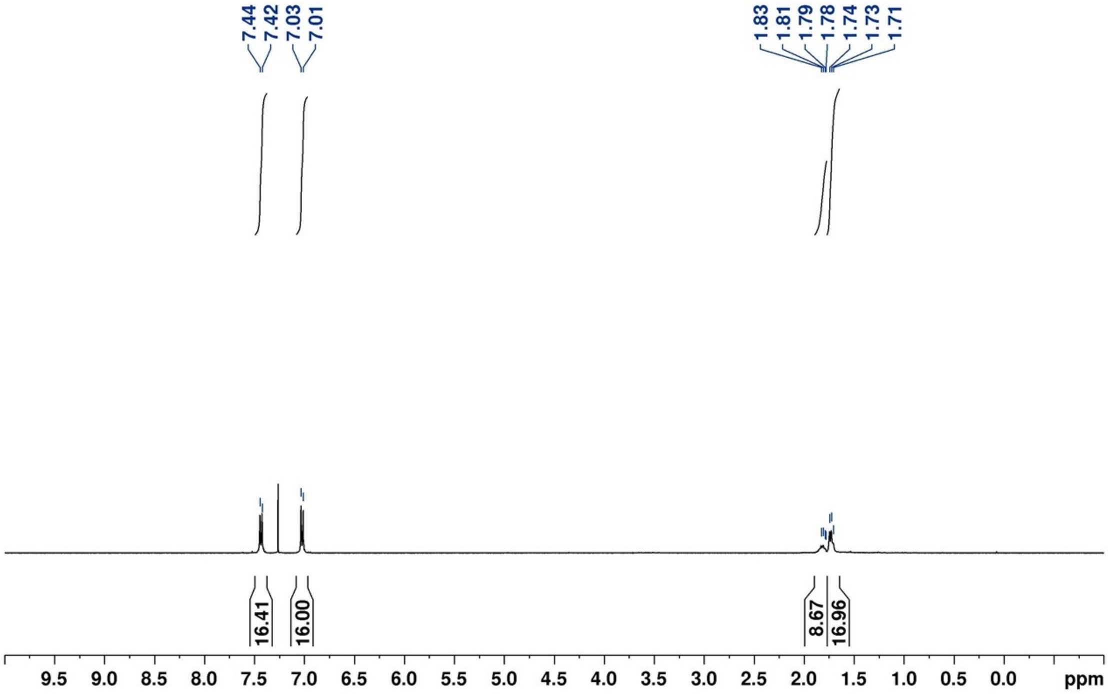

Figure S21. ^{1}H NMR spectrum of **2** in $CDCl_3$ (400 MHz).

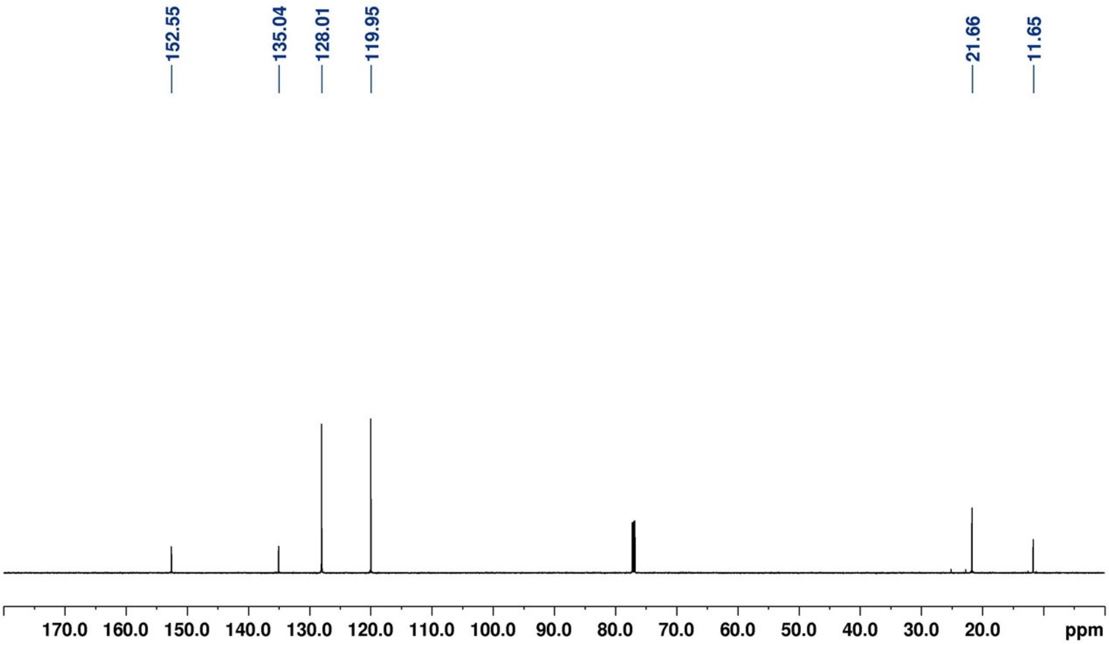

F

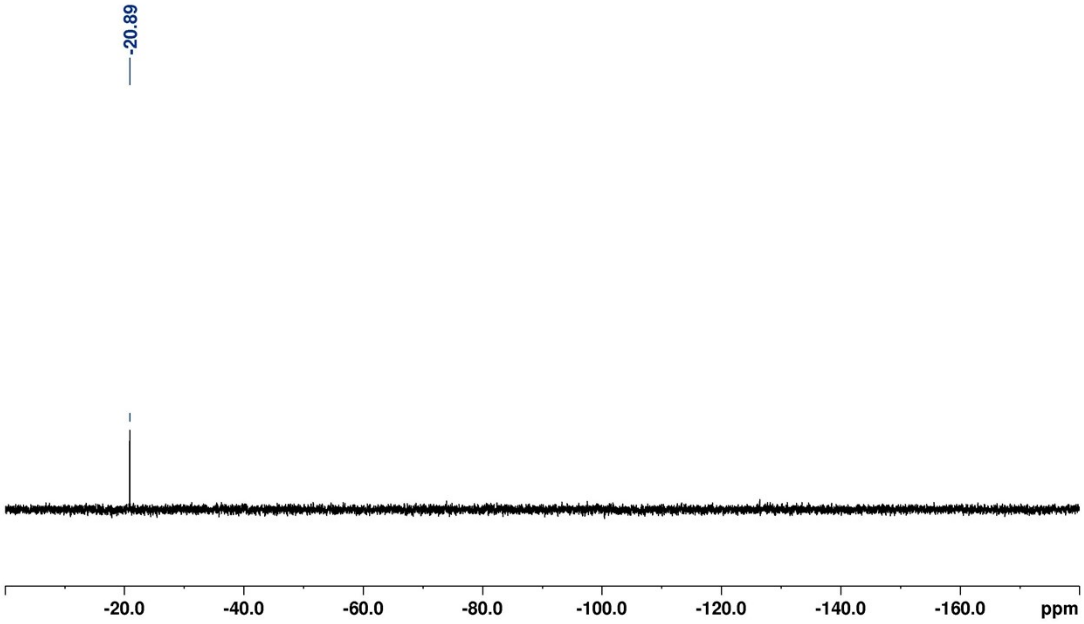

Figure S23. ^{29}Si DEPT NMR spectrum of **2** in CDCl$_3$ (79 MHz).

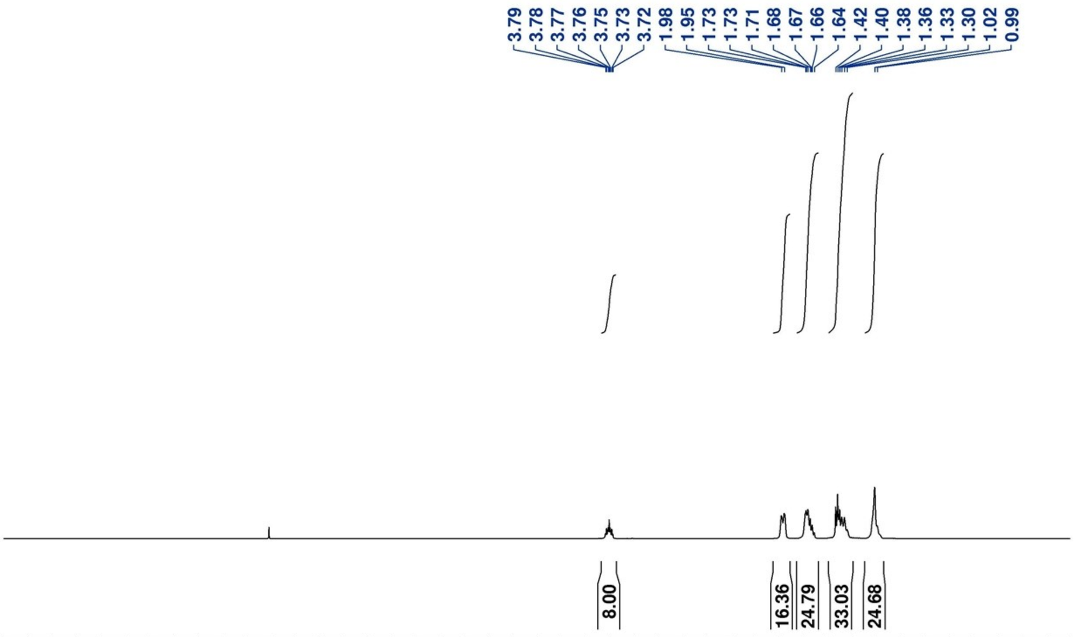

Figure S24. ^{1}H NMR spectrum of **4** in CDCl$_3$ (400 MHz).

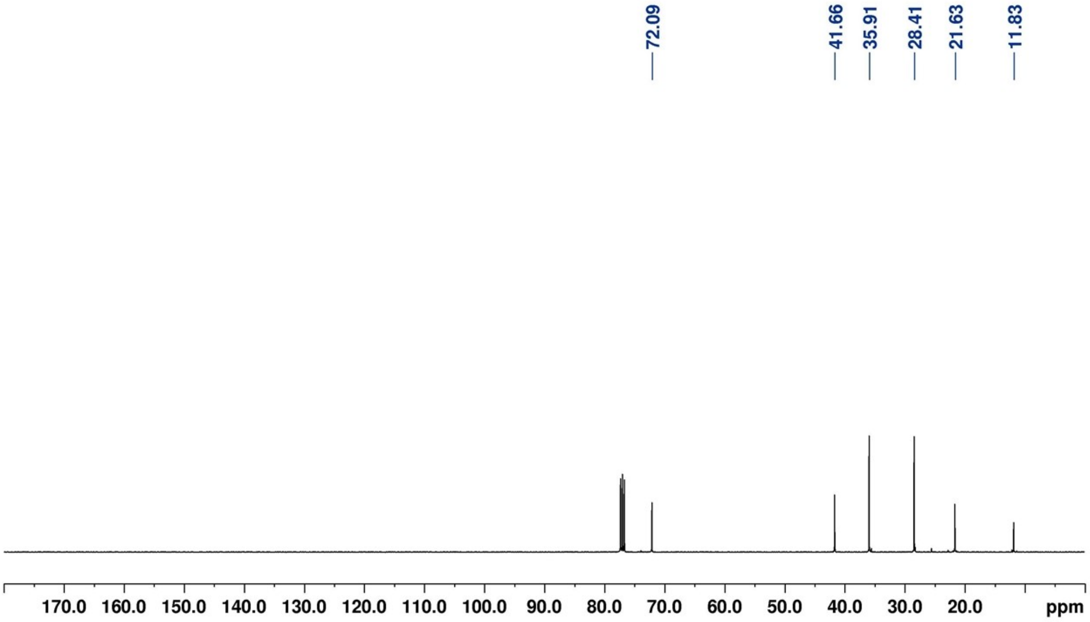

Figure S25. $^{13}C\{^{1}H\}$ NMR spectrum of **4** in $CDCl_3$ (100 MHz).

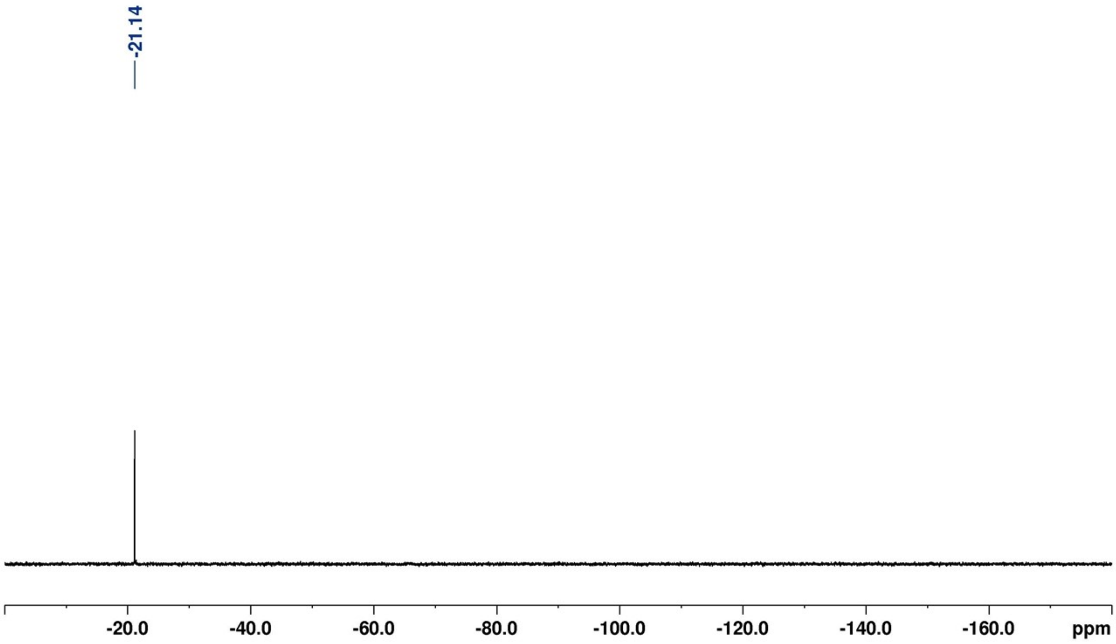

Figure S26. ^{29}Si DEPT NMR spectrum of **4** in $CDCl_3$ (79 MHz).